processes

MDPI

Article

Exergy and Environmental Analysis for Optimal Condition Finding of a New Combined Cycle

Ibrahim B. Mansir [1,2]

[1] Mechanical Engineering Department, College of Engineering in Al-Kharj, Prince Sattam bin Abdulaziz University, Al-Kharj 11942, Saudi Arabia; i.balarabe@psau.edu.sa
[2] Centre for Energy Research and Training, Ahmadu Bello University, Zaria P.M.B 1045, Nigeria

Abstract: In this paper, various thermal energy systems are studied to recover waste heat from gas turbines with different configurations. The exergy analysis and environmental examination are applied to achieve better insight into the suggested systems. Also, multi-objective optimization is employed to find the optimal condition of the introduced plants. In this work, various systems such as gas turbine (GT), organic Rankine cycle (ORC), and Kalina cycle (KC) with Proton Exchange Membrane (PEM) electrolyzer are combined to achieve a new system design. In this study, Engineering Equation Solver (V11.755) and Matlab (R2023a) software are used to simulate and optimize the proposed system. The comparison of systems shows that the combustion chamber with 3622 kW has the most considerable exergy destruction in the IGT/ORC-KC plant. The comparative investigation shows that IGT/ORC-KC has the highest output at 5659 kW, while the smallest exergy destruction is associated with the IGT system with 1779 kW. The multi-objective optimization considering three objective functions, namely, exergy efficiency, product cost, and environmental effects of exergy destruction, is conducted. Three-objective optimization on the IGT/ORC-KC unit shows that in the optimum point selected by the Technique for Order of Preference by Similarity to Ideal Solution (TOPSIS) approach, the exergy efficiency, cost of product, and environmental effect of exergy destruction rate are 29.5%, 0.31 USD/kWh, and 13.22 mPt/s.

Keywords: intercooled gas turbine; exergo-economic; Kalina cycle; optimization; energy recovery

Citation: Mansir, I.B. Exergy and Environmental Analysis for Optimal Condition Finding of a New Combined Cycle. *Processes* **2024**, *12*, 312. https://doi.org/10.3390/pr12020312

Academic Editor: Blaž Likozar

Received: 14 January 2024
Revised: 30 January 2024
Accepted: 30 January 2024
Published: 1 February 2024

1. Introduction

Due to population increments and the increase in the need for energy at the global level, the issue of energy management has received particular attention today because the excessive consumption of energy sources, including fossil fuels, reduces these resources and also causes air pollution; the environmental damage caused by this event leads people to reconsider the existing approaches of energy generation, consumption, and storage [1].

The most crucial energy carriers needed to meet the needs of modern life are natural gas and electricity because they can be easily exploited. Also, many devices and types of equipment are dependent on electricity and natural gas. Due to the dependencies between natural gas and electricity, the integrated exploitation of these sources increases the reliability of the energy supply. Combining systems and switching between different energies using the unique advantages of each of them can lead to favorable results [2]. On the other hand, integrated energy systems can promote the efficiency of energy consumption and economic benefit [3,4]. The integrated energy system is a promising option for transferring and storing different energies, which is an intermediary between the supplier, consumer, and energy transmission infrastructure and can be used to optimize the energy network [5].

Gas turbines are one of the most important power generation machines in today's industry and play an essential role in the production of constant electricity. For various reasons, they will have an essential place in power generation. Therefore, with the increase in the share of gas power plants in the production and supply of electricity, and also in

order to optimize the use of existing energy resources, gas turbines are always at the center of attention. Until now, due to operational costs and greenhouse gas emissions, there has been extensive effort to improve the efficiency of gas turbines. The emission of greenhouse gases from gas turbines is relatively high compared to that of other power plants. The exhaust of the gas turbine has high potential, and it can increase the production capacity of the waste heat recovery (WHR) boiler.

Due to the flow rate and high temperature of the exhaust gas, the total thermal efficiency of the gas turbine is relatively low. One way to increase power plants' efficiency is to combine different cycles [6,7]. Based on this, energy and exergy analysis has become an important tool for designing, analyzing, and developing combined systems based on gas turbine units. The energy efficiency is usually not complete in the investigation of thermodynamic cycles, because it does not give an accurate measure of the system's operation to reach the ideal state. In addition, the thermodynamic losses that occur in a system usually cannot be accurately identified by energy examination. Hence the exergy, exergo-economic, and exergo-environmental analyses are a suitable approach for the more optimal use of energy resources, by which the location, cause, and actual losses in power plant cycles can be determined both quantitatively and qualitatively. The development of integrated energy systems is widely addressed because of their high efficiency [8]. Therefore, the latest studies in this field will be discussed.

In a study, Hosseini [9] investigated the performance of a GT power generation plant with biogas fuel integrated with a flameless boiler to generate steam to produce hydrogen in a solid oxide steam electrolysis. The results of this study showed that by purifying biogas and increasing the concentration of methane to 80%, the electric power and hydrogen produced increased by 24% and 20%, respectively. Also, the inlet temperature of the GT should be set at temperatures higher than 1300 K in order to provide favorable conditions for the operation of the boiler without flame.

Nami et al. [10] examined an integrated energy plant to retrieve the dissipated heat of a GT to drive an ORC for hydrogen generation using a PEM electrolyzer. Their work showed that the exergy efficiency and hydrogen generation rates were 49.21% and 56.2 kg/h. Also, in a similar study, Nami and Akrami [11] assessed a hybrid plant including a GT and PEM electrolysis from the perspective of exergy and exergo-economics. It was concluded that the exergy efficiency and hydrogen production rate were 52.09% and 8.723 kg/h.

Singh et al. [12] investigated a hybrid biomass–gas turbine integrated with a solid oxide fuel cell (SOFC-GT) and an ORC. They examined the influences of different performance parameters of the GT and ORC. Their study showed that by retrieving the waste energy of the SOFC-GT cycle via the ORC, the efficiency increases by about 8–12%. Also, Khoshgoftar Menesh et al. [13] proposed and evaluated a new combination of a GT with an ORC and a multi-effect desalination unit. The exergy, exergo-environmental, and exergo-economic analyses were carried out. It was concluded that the suggested combined system can generate 5000 m^3/day of fresh water. In addition, the energy and exergy efficiency of the studied system was reported to be 47.85% and 41.94%, which had 11.6% and 3.6% enhancement compared to the integrated gas turbine and solid oxide fuel cell system.

In another work, Gholamian et al. [14] investigated the multi-objective optimization of an integrated biomass-fed GT and hydrogen generation through electrolysis. The research aimed to use the WHR in a biomass-based SOFC considering multi-objective optimization based on the exergy efficiency and total product cost as objective functions. Also, Shamoushaki et al. [15] studied a multi-objective optimization for an integrated energy system based on the biomass and gas turbine (SOFC/GT). Findings showed that at the optimal point, the total cost rate and exergy efficiency of the plant were 0.0435 USD/s and 57.7%, respectively.

Hemadri and Subbarao [16] investigated the thermal integration of a reheat ORC (RH-ORC) with GT for maximum power recovery. This study considered cyclopentane, hexane, and benzene as working fluids. It was reported that the net output of the plant increased with reheating. Musharavati et al. [4] investigated WHR in an intercooled GT unit with

thermo-economic approaches and conducted three-objective optimization. The primary purpose of the studied plant was to improve the thermodynamic and exergo-economic operation along with multi-objective optimization, which led to improving the stability of the plant. Abd El-Sattar et al. [17] examined a GT combined plant with an ORC and a chiller to produce about 170 kW of electricity from 144 kg/h of biogas fuel. In this study, according to the boiling temperature of the working agent and the temperature of the heat resource, toluene was chosen as a suitable working fluid in the ORC. The results of this study showed that the total electrical power, cooling, and efficiency were 177.56 kW, 38.5 kW, and 24.4%. Roy et al. [18] studied the economic and environmental analysis of a GT unit combined with SOFC and ORC. The thermodynamics and economics of the system were examined under different operating conditions. The results of this study showed that the energy and exergy efficiencies of the proposed plant were 49.47% and 44.2%. It was concluded that the system operates better in terms of efficiency and cost of electricity than the conventional system. In another study conducted by Cao et al. [19], a new biomass-fueled GT was introduced. The waste heat of the GT was used to generate electricity through an ORC and the cooling of the inlet of the gas turbine compressor through the absorption cooling cycle was performed. In multi-objective optimal points, the gas turbine system with inlet cooling had 11.2% higher exergy efficiency and 12.3% lower electricity cost than the gas turbine system with organic Rankine cycle.

The energy, exergy, economic, and environmental (4E) analyses of an integrated biomass-fueled micro gas turbine (MGT) energy system with a superheated Kalina cycle (SKC) were evaluated by Liu et al. [20]. From energy and exergy points of view, the SKC integration with the MGT improved the system energy and exergy efficiency from 30.7% and 26.1% to 51.7% and 50.8%, respectively. Ebrahimi-Moghadam et al. [21] evaluated an integrated energy system from the perspectives of energy, exergy, exergo-economics, and exergo-environmental factors. To recover waste heat, a GT, a heat exchanger for the heating part, a Kalina cycle to produce additional power, and an ejector refrigeration system to produce cooling were employed. The optimal values of energy efficiency, exergy efficiency, exergo-economic parameters, and exergo-environment parameters were 76.9%, 30.8%, 58.4 USD/GJ, and 42.7 kg/GJ. In a study, Du et al. [22] investigated the multi-objective optimization of a hybrid plant according to the GT with compressor precooling, a Kalina cycle, and an ejector refrigeration unit (GT-KCS-ERC). Thermodynamic and thermo-economic analyses were performed to show the feasibility of the new hybrid plant compared with the stand-alone system (GT-KCS). It was concluded that the energy efficiency of GT-KCS-ERC increases with the enhancement in the boiler pinch point and the decrease in the ammonia concentration of the workings in the KCS, while in the GT-KCS the opposite trend was observed. Mohammadkhani et al. [23] examined the exergo-economic analysis of WHR from a 98.9 kW engine using the Kalina cycle. Energy and exergy efficiencies were 25.55% and 55.52%, and the cost of the unit of power produced in the Kalina plant was 15.52 cent/kWh. In addition, the unit cost of generated power and the cost of the entire plant were reduced by enhancing turbine inlet temperature and pressure.

The energy crisis is a crucial issue for many countries today. One way to overcome the energy crisis is by enhancing the efficiency of energy conversion and reducing waste energy. In the continuation of the work previously performed, in this article, the GT cycle is investigated using the ORC and the Kalina cycle and the thermoelectric module and PEM electrolysis for hydrogen production. Also, by defining the appropriate objective functions, multi-objective optimization is performed based on the exergy, economic, and exergo-environmental analysis for the introduced system. The primary novel parts of this work are introducing various GT-based systems integrated with the Kalina cycle and PEM electrolysis to generate hydrogen and comparing these systems. Besides the exergy-environmental analysis, a new method is applied to the introduced system to assess the suggested plant.

2. Layouts

The proposed plant in this article is designed based on a gas turbine equipped with an intermediate cooler. Three systems are studied in Figure 1a–c. Figure 1a,b illustrate the basic gas turbine with the intercooler and the basic system with the Kalina cycle, respectively. In the suggested system (Figure 1c), an organic Rankine cycle is used by applying intermediate cooling heat to start the system, and a Kalina cycle is used to minimize waste heat at the gas turbine outlet. In the suggested configuration, in the condenser section of the Kalina cycle, to convert the useless heat of the condenser discharging to the environment, a thermoelectric generator is used. Also, an electrolyzer has been used to convert part of the electrical energy into hydrogen and at the same time to store it in storage tanks. The proposed system recovers the heat from the wastes of the gas turbine cycle through the organic Rankine cycle and the Kalina cycle in three sections.

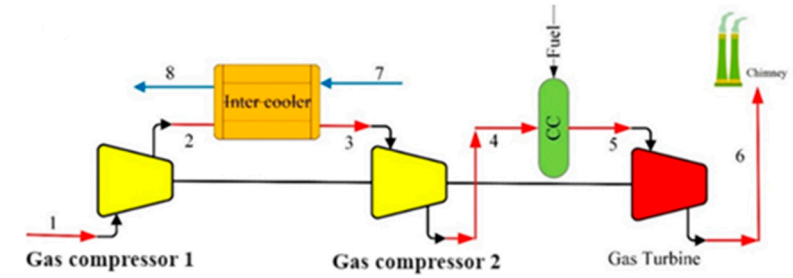

(**a**)

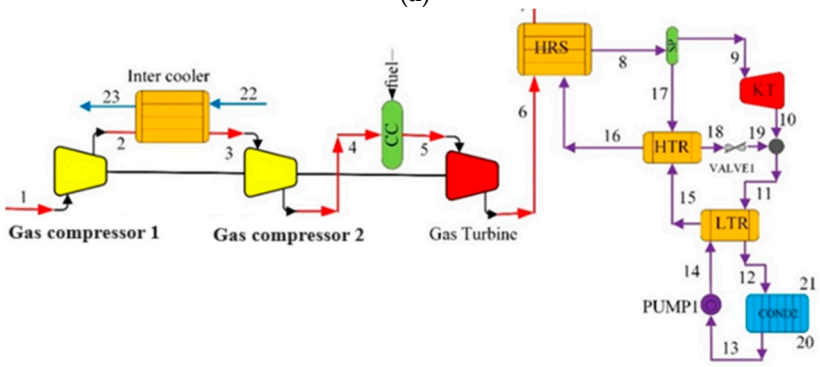

(**b**)

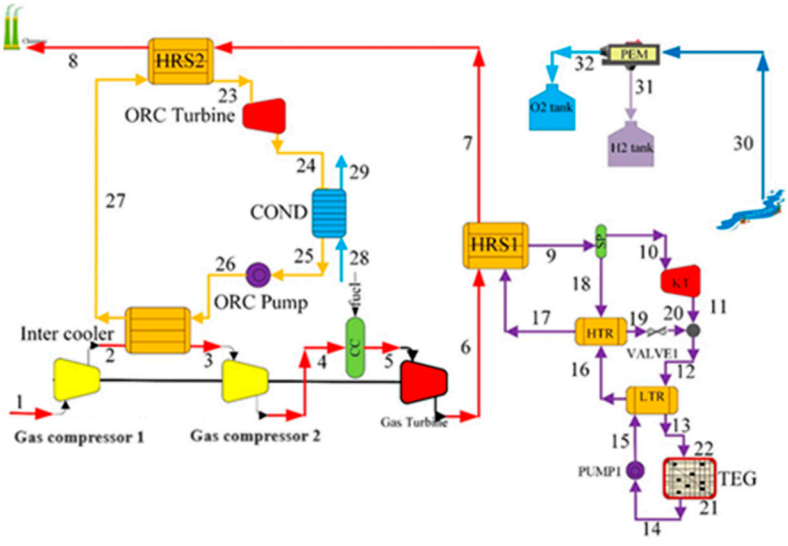

(**c**)

Figure 1. The schematic diagram of the studied systems with intercooler gas turbine: (**a**) IGT, (**b**) IGT/KC, and (**c**) IGT/ORC-KC.

3. Methodology

3.1. Energy Model

The essential equations of thermodynamics are the mass and energy conservation equations that must be written for each part of the system to simulate the behavior. To simplify the models, the assumptions should be taken into account as follows:

- All processes have been examined in the steady-state mode.
- The operating temperature of the PEM electrolyzer is considered 85 °C.
- The efficiencies of the compressor and the gas turbine are considered to be 0.85 and 0.9, respectively.
- The combustion chamber efficiency is considered to be 95%.

According to the mass conservation law, mass is an infinite property of matter that remains constant in the chemical changes of matter. The mass conservation law can be written as follows for a control volume in the steady-state condition:

$$\sum_{in} \dot{m}_{in} = \sum_{out} \dot{m}_{out} \tag{1}$$

In the above equation, $\dot{m}$ is usually expressed in kg/s.

According to the conservation of energy, energy is neither produced nor destroyed, but it is always converted from one form to another. In the steady states, the energy conservation law or the first thermodynamics law is written as follows [24]:

$$\dot{Q}_{in} + \dot{W}_{in} + \sum_{in} \dot{m}_{in} h_{in} = \dot{Q}_{out} + \dot{W}_{out} + \sum_{out} \dot{m}_{out} h_{out} \tag{2}$$

3.2. Exergy Analysis

Exergy is a property that shows the ability to perform the useful work of a system with the specific value of energy in a specific condition. The balance of exergy for a volume of control can be written as follows:

$$\dot{E}x_f = \dot{E}x_p + \dot{E}x_D + \dot{E}x_L \tag{3}$$

The exergy loss in the above equation is written as follows:

$$\dot{E}x_L = \left(1 - \frac{T_0}{T}\right) \dot{Q}_{loss} \tag{4}$$

In the above equation, $\dot{Q}_{loss}$ is the lost heat of the control volume. Also, in Table 1 the energy and exergy balance equations are given for each volume of controls.

To achieve the system assessment, the following relation is used:

$$\begin{aligned} \dot{E}x_d = {} & \dot{E}_{D,IC} + \dot{E}_{D,comp1} + \dot{E}_{D,comp2} + \dot{E}_{D,CC} + \dot{E}_{D,GT} + \dot{E}_{D,HRS1} + \dot{E}_{D,T,ORC} + \dot{E}_{D,cond} + \dot{E}_{D,P,ORC} \\ & + \dot{E}_{D,sep} + \dot{E}_{D,KT} + \dot{E}_{D,TEG} + \dot{E}_{D,Valve} + \dot{E}_{D,HTR} + \dot{E}_{D,LTR} + \dot{E}_{D,P} + \dot{E}_{D,HRS2} \\ & + \dot{E}_{D,PEM,elec} \end{aligned} \tag{5}$$

$$\dot{W}_{net} = \dot{W}_{KT} + \dot{W}_{gas\ tur} + \dot{W}_{ORC,T} + \dot{W}_{TEG} - \dot{W}_{KP} - \dot{W}_{ORC,P} - \dot{W}_{comp1} - \dot{W}_{comp2} - \dot{W}_{PEM,elec} \tag{6}$$

$$\eta_{en} = \frac{\dot{W}_{net} + \dot{m}_{H_2} * LHV_{H_2}}{\dot{m}_{fuel} * LHV_{fuel}} \tag{7}$$

$$\eta_{ex} = \frac{\dot{W}_{net} + \dot{m}_{H_2} * \dot{E}_{H_2}}{\dot{m}_{fuel} * \dot{E}_{fuel}} \tag{8}$$

Table 1. Energy and exergy relations for the system components.

Elements	Energy	Exergy Destruction
Intercooler	$\dot{Q}_{IC} = \dot{m}_2(h_2 - h_3) = \dot{m}_{ORC}(h_{27} - h_{26})$	$\dot{E}_{D,IC} = (\dot{E}_2 - \dot{E}_3) - (\dot{E}_{26} - \dot{E}_{27})$
Compressor 1	$\dot{W}_{comp1} = \dot{m}_1(h_2 - h_1)$	$\dot{E}_{D,comp1} = (\dot{E}_1 - \dot{E}_2) + \dot{w}_{comp1}$
Compressor 2	$\dot{W}_{comp2} = \dot{m}_3(h_4 - h_3)$	$\dot{E}_{D,comp2} = (\dot{E}_3 - \dot{E}_4) + \dot{w}_{comp2}$
CC	$\dot{Q}_{CC} = \dot{m}_4 h_4 + \dot{m}_{fuel} LHV = \dot{m}_5 h_5 + (1 - \eta_{cc}) * \dot{m}_{fuel} LHV$	$\dot{E}_{D,CC} = \left(\dot{E}_4 - \dot{E}_5\right) + \dot{m}_{fuel} LHV * 1.06$
Gas Turbine	$\dot{W}_{GT} = \dot{m}_5(h_5 - h_6)$	$\dot{E}_{D,GT} = (\dot{E}_5 - \dot{E}_6) - \dot{w}_{GT}$
HRS1	$\dot{Q}_{HRS1} = \dot{m}_6(h_6 - h_7) = \dot{m}_{17}(h_{17} - h_9)$	$\dot{E}_{D,HRS1} = (\dot{E}_6 - \dot{E}_7) - (\dot{E}_9 - \dot{E}_{17})$
ORC Turbine	$\dot{W}_{T,ORC} = \dot{m}_{ORC}(h_{23} - h_{24})$	$\dot{E}_{D,T,ORC} = (\dot{E}_{23} - \dot{E}_{24}) - \dot{w}_{ORC,T}$
Condenser	$\dot{Q}_{cond} = \dot{m}_{24}(h_{24} - h_{25}) = \dot{m}_{29}(h_{29} - h_{28})$	$\dot{E}_{D,cond} = (\dot{E}_{24} - \dot{E}_{25}) - (\dot{E}_{28} - \dot{E}_{29})$
ORC Pump	$\dot{W}_{P,ORC} = \dot{m}_{ORC}(h_{26} - h_{25})$	$\dot{E}_{D,P,ORC} = (\dot{E}_{25} - \dot{E}_{26}) + \dot{w}_p$
Separator	$\dot{m}_9 h_9 = \dot{m}_{18} h_{18} + \dot{m}_{10} h_{10}$	$\dot{E}_{D,sep} = \dot{E}_9 - \dot{E}_{18} - \dot{E}_{10}$
Kalina Turbine	$\dot{W}_{KT} = \dot{m}_{10}(h_{10} - h_{11})$	$\dot{E}_{D,KT} = (\dot{E}_{10} - \dot{E}_{11}) - \dot{w}_{KT}$
Thermoelectric	$\dot{Q}_{TEG} = \dot{m}_{13}(h_{13} - h_{14}) = \dot{m}_{22}(h_{22} - h_{21})$	$\dot{E}_{D,TEG} = (\dot{E}_{13} - \dot{E}_{14}) - (\dot{E}_{21} - \dot{E}_{22}) - \dot{w}_{teg}$
Valve	$h_{19} = h_{20}$	$\dot{E}_{D,Valve} = \dot{E}_{19} - \dot{E}_{20}$
HTR	$\dot{Q}_{HTR} = \dot{m}_{16}(h_{16} - h_{17}) = \dot{m}_{18}(h_{19} - h_{18})$	$\dot{E}_{D,HTR} = (\dot{E}_{16} - \dot{E}_{21}) - (\dot{E}_{18} - \dot{E}_{19})$
LTR	$\dot{Q}_{LTR} = \dot{m}_{12}(h_{12} - h_{13}) = \dot{m}_{15}(h_{16} - h_{15})$	$\dot{E}_{D,LTR} = (\dot{E}_{12} - \dot{E}_{13}) - (\dot{E}_{15} - \dot{E}_{16})$
Pump	$\dot{W}_P = \dot{m}_{14}(h_{14} - h_{15})$	$\dot{E}_{D,P} = (\dot{E}_{14} - \dot{E}_{15}) + \dot{w}_p$
HRS2	$\dot{Q}_{HRS2} = \dot{m}_7(h_7 - h_8) = \dot{m}_{23}(h_{23} - h_{27})$	$\dot{E}_{D,HRS2} = (\dot{E}_7 - \dot{E}_8) - (\dot{E}_{27} - \dot{E}_{23})$

LTR: low temperature heat exchanger; HTR: high temperature heat exchanger.

3.3. Exergo-Economic Model

Exergo-economics are a part of engineering that mixes economic and thermodynamic concepts. Deciding on the system's performance requires information obtained by using cost balance. In the exergo-economic examination, the cost balance of the system component can be obtained as follows [25]:

$$\dot{C}_p = \dot{C}_F + \dot{Z}_{CI} + \dot{Z}_{O\&M} \tag{9}$$

Here, $\dot{C}_f$ and $\dot{C}_p$ show the cost rate of fuel and products. Also, $\dot{Z}_{CI}$ and $\dot{Z}_{O\&M}$ represent the capital investment cost and the operation and maintenance cost. Table 2 shows the cost balance and auxiliary equations.

Table 2. The cost balance and auxiliary equations.

Components	Cost Balance	Auxiliary Equation
Intercooler	$\dot{C}_{27} + \dot{C}_3 = \dot{C}_2 + \dot{C}_{26} + \dot{Z}_{IC}$	$c_2 = c_3$
CC	$\dot{C}_5 = \dot{C}_4 + \dot{C}_{feul} + \dot{Z}_{cc}$	-
Compressor 1	$\dot{C}_2 = \dot{C}_1 + \dot{Z}_{comp1} + \dot{C}_{w,comp1}$	$c_{w,comp1} = c_{w,GT}$
Compressor 2	$\dot{C}_4 = \dot{C}_3 + \dot{Z}_{comp2} + \dot{C}_{w,comp2}$	$c_{w,comp2} = c_{w,GT}$
HRS1	$\dot{C}_7 + \dot{C}_9 = \dot{C}_6 + \dot{C}_{17} + \dot{Z}_{hrs1}$	$c_6 = c_7$
Gas Turbine	$\dot{C}_6 + \dot{C}_{w,gt} = \dot{C}_5 + \dot{Z}_{gt}$	$c_5 = c_6$
Condenser	$\dot{C}_{25} + \dot{C}_{29} = \dot{C}_{24} + \dot{C}_{28} + \dot{Z}_{cond}$	$c_{24} = c_{25}$
ORC Turbine	$\dot{C}_{24} + \dot{C}_{w,orct} = \dot{C}_{23} + \dot{Z}_{orct}$	$c_{23} = c_{24}$
ORC Pump	$\dot{C}_{26} = \dot{C}_{25} + \dot{Z}_{orcp} + \dot{C}_{w,orcp}$	$c_{w,orcp} = c_{w,orct}$
Separator	$\dot{C}_9 = \dot{C}_{10} + \dot{C}_{18}$	$c_{10} = c_{18}$
Kalina Turbine	$\dot{C}_{11} + \dot{C}_{w,kt} = \dot{C}_{10} + \dot{Z}_{kt}$	$c_{10} = c_{11}$
Thermoelectric	$\dot{C}_{14} + \dot{C}_{22} + \dot{C}_{w,teg} = \dot{C}_{21} + \dot{C}_{13} + \dot{Z}_{teg}$	$\frac{\dot{c}_{13} - \dot{c}_{14}}{\dot{E}_{13} - \dot{E}_{14}} = \frac{\dot{c}_{21} - \dot{c}_{22}}{\dot{E}_{21} - \dot{E}_{22}}$ $c_{21} = 0,\ c_{13} = c_{14}$

Table 2. *Cont.*

Components	Cost Balance	Auxiliary Equation
Valve	$\dot{C}_{19} = \dot{C}_{20}$	–
HTR	$\dot{C}_{17} + \dot{C}_{19} = \dot{C}_{16} + \dot{C}_{18} + \dot{Z}_{HTR}$	$c_{18} = c_{19}$
LTR	$\dot{C}_{13} + \dot{C}_{16} = \dot{C}_{12} + \dot{C}_{15} + \dot{Z}_{LTR}$	$c_{12} = c_{13}$
Pump	$\dot{C}_{15} = \dot{C}_{14} + \dot{Z}_p + \dot{C}_{w,p}$	$c_{w,p} = c_{w,kt}$
HRS2	$\dot{C}_8 + \dot{C}_{23} = \dot{C}_{27} + \dot{C}_7 + \dot{Z}_{hrs2}$	$c_7 = c_8$

3.4. Exergo-Environmental Model

Exergo-environmental analysis includes three stages of analysis. The first step is to perform an exergy examination of the system. In the second step, a life cycle assessment is performed. In the last step, the environmental effects obtained from the life cycle assessment are assigned to the exergy flows in the system. With the help of this evaluation, the most important system component with the highest environmental impact will be determined [26].

3.4.1. Life Cycle Assessment

Life cycle assessment is a fundamental approach to assessing the influences of a product on the environment during its life cycle. The process of life cycle assessment includes the definition of the system, the identification of the amount of consumption and the amount of release of materials, and finally the analysis of the results. The life cycle rate is calculated by Simapro software (Version 9.4) based on international standards [27].

3.4.2. Exergo-Environmental Analysis

In order to perform an environmental analysis, an environmental impact rate $\dot{B}_j$ and environmental impact per exergy unit b_j must be defined. The environmental effect rate $\dot{B}_j$ is the environmental effects of points per time unit (Pts/h or mPts/h) in the environmentally friendly index. Specific environmental impact (based on exergy) b_j (which is also defined as specific environmental cost) is the average environmental influences related to the production of flow j per unit of exergy of the same flow. The environmental influence rate $\dot{B}_j$ of flow j is the product of the exergy rate of that flow $\dot{E}x_j$ and the specific environmental effect b_j:

$$\dot{B}_j = b_j \dot{E}x_j \tag{10}$$

$$\dot{B}_q = b_q \dot{E}x_q \tag{11}$$

$$\dot{B}_w = b_w \dot{E}x_w \tag{12}$$

3.4.3. Exergo-Environmental Balance

The balance of system environmental impact relationships is written for each element of the system. The basis of the formulation in the balance of environmental effects is that the environmental effects entered into the system component must be removed from the same system component by the output flow. In addition to the environmental effects related to the input flow, the environmental effects related to the system component $\dot{Y}_k$, related to the life cycle of the k^{th} system component, also play a role in the balance, the relationship of which is as follows [28]:

$$\dot{Y}_k = \dot{Y}_k^{CO} + \dot{Y}_k^{O\&M} + \dot{Y}_k^{DI} \tag{13}$$

where $\dot{Y}_k^{CO}$, $\dot{Y}_k^{O\&M}$, $\dot{Y}_k^{DI}$ are related to construction, operation and maintenance, and disposal of waste and constitute the component associated to environmental impact. The exergo-environmental balance for the component is as follows [29]:

$$\sum_{j=1} \dot{B}_{j,k,in} + \dot{Y}_k = \sum_{j=1} \dot{B}_{j,k,out} \quad (14)$$

In Table 3 the environmental effect balance with the auxiliary equation is presented.

Table 3. The environmental influences balance and auxiliary equations.

Components	Environment Effect Balance	Auxiliary Equation
Intercooler	$\dot{B}_{27} + \dot{B}_3 = \dot{B}_2 + \dot{B}_{26} + \dot{Y}_{IC}$	$b_2 = b_3$
CC	$\dot{B}_5 = \dot{B}_4 + \dot{Y}_{CC} + \dot{B}_{fuel}$	–
Compressor 1	$\dot{B}_2 = \dot{B}_1 + \dot{Y}_{comp1} + \dot{B}_{comp1}$	$B_{comp1} = B_{GT}$
Compressor 2	$\dot{B}_4 = \dot{B}_3 + \dot{Y}_{comp2} + \dot{B}_{comp2}$	$B_{comp2} = B_{GT}$
HRS1	$\dot{B}_7 + \dot{B}_9 = \dot{B}_{17} + \dot{Y}_{HRS1} + \dot{B}_6$	$b_6 = b_7$
Gas Turbine	$\dot{B}_6 + \dot{B}_{GT} = \dot{B}_5 + \dot{Y}_{GT}$	$b_5 = b_6$
Condenser	$\dot{B}_{25} + \dot{B}_{29} = \dot{B}_{24} + \dot{B}_{28} + \dot{Y}_{cond}$	$b_{24} = b_{25}$
ORC Turbine	$\dot{B}_{24} + \dot{B}_{orct} = \dot{B}_{23} + \dot{Y}_{orct}$	$b_{23} = b_{24}$
ORC Pump	$\dot{B}_{26} = \dot{B}_{25} + \dot{Y}_{orcp} + \dot{B}_{orcp}$	$B_{orcp} = B_{orct}$
Separator	$\dot{B}_{18} + \dot{B}_{10} = \dot{B}_9$	$b_{17} = b_9$
Kalina Turbine	$\dot{B}_{10} + \dot{Y}_{kt} = \dot{B}_{11} + b_{power} * \dot{w}_{kt}$	$b_{10} = b_{11}$
Thermoelectric	$\dot{B}_{14} + \dot{B}_{22} + \dot{B}_{teg} = \dot{B}_{21} + \dot{B}_{13} + \dot{Y}_{teg}$	$\frac{\dot{B}_{13} - \dot{B}_{14}}{\dot{E}_{13} - \dot{E}_{14}} = \frac{\dot{B}_{21} - \dot{B}_{22}}{\dot{E}_{21} - \dot{E}_{22}}$ $b_{21} = 0 \;\; b_{13} = b_{14}$
Valve	$\dot{B}_{19} = \dot{B}_{20}$	–
HTR	$\dot{B}_{17} + \dot{B}_{19} = \dot{B}_{16} + \dot{B}_{18} + \dot{Y}_{HTR}$	$b_{18} = b_{19}$
LTR	$\dot{B}_{13} + \dot{B}_{16} = \dot{B}_{12} + \dot{B}_{15} + \dot{Y}_{LTR}$	$b_{12} = b_{13}$
Pump	$\dot{B}_{15} = \dot{B}_{14} + \dot{B}_p + \dot{Y}_p$	$B_p = B_{kt}$
HRS2	$\dot{B}_8 + \dot{B}_{23} = \dot{B}_{27} + \dot{B}_7 + \dot{Y}_{hrs2}$	$b_7 = b_8$

4. Results and Discussion

In the following sections, the results of the simulation are presented. To validate the prepared code, a verification was conducted on the obtained results. Additionally, the results of the thermodynamic analysis and the exergy, exergo-economic, and exergo-environmental analysis is reported. Also, a comparison with basic cycles is presented.

4.1. Validation

In the current section, the results of the prepared model and references are presented. Considering that the validity of the analysis is highly dependent on the validity of the prepared code, the results of the prepared calculation code are validated at first in the EES software. As shown in Tables 4 and 5, the presented results of the modeling of the current study illustrate an insignificant difference compared to the results of the references from Refs. [30,31].

Table 4. The results of the Brayton cycle validation.

Stream Brayton Cycle	P (bar)		T (°C)		h (kJ/kg)	
	Present Work	Ref. [30]	Present Work	Ref. [30]	Present Work	Ref. [30]
1	1.01	1.01	25	25	298.4	302.86
2	3.194	3.19	161	161.73	435.8	447.61
3	3.194	3.16	40	40	313.1	319.25
4	10.1	10	184.6	184.44	459.5	474.33
5	10.1	10	800	800	1131	1250.65
6	1.01	1.04	392.1	391.97	676.6	730.15
7	1.01	1.02	200	217.83	475.9	514.59

Table 5. The results of the Kalina cycle validation.

Stream Kalina Cycle	P (bar)		T (°C)	
	Present Research	Ref. [31]	Present Research	Ref. [31]
9	25	25	90	90
10	25	25	90	90
11	11.44	12.4	48.5	52.6
12	11.44	12.4	53.2	57.8
13	11.44	12.16	49.6	53.7
14	11.44	12.16	35	37
15	25	26.79	35.4	37.4
16	25	26.27	47.5	47.8
17	25	25.5	59	59.3
18	25	25	90	90
19	25	24.25	58.1	57.8
20	11.44	12.4	56.7	57.9

4.2. Results of the Developed System

By solving the equations of mass, energy, and entropy balance for each component of the studied system, the pressure, temperature enthalpy, and entropy can be measured at different points of the proposed cycle. This would effectively obtain the amount of work and heat exchanged in each part of the system.

4.2.1. Exergy and Exergo-Economic Analysis

Exergy analysis can help identify the most inefficient element of the system in terms of the second law of thermodynamics. Here, the results of the calculation for the IGT/ORC-KC will be developed. The diagram in Figure 2a shows the exergy destruction in various elements of system 3 (the suggested system). The combustion chamber is assigned a significant amount of exergy destruction to itself with 3622 kW, and after that, HRS1 is in second place with 674.2 kW. Moreover, Figure 2b shows the contribution of each part of the system to the total exergy destruction. The results reveal that the combustion chamber has over half of the total exergy destruction.

To better understand the exergy flow in the subsystems that make up the IGT/ORC-KC integrated system, the exergy flow is shown in the Sankey diagram in Figure 3. In addition, Table 6 shows the complete results of the exergo-economic examination along with the exergo-economic parameters required in the system examination. The last column shows the relative cost difference for each element. The high value of this parameter indicates the cost of increasing exergy in that component. Considering the high cost of increasing the exergy flow in the HRS1 element, the parameter of r_k for this component is higher than the others.

Table 6. The exergo-economic parameters for the IGT/ORC-KC system.

Component	$\dot{E}x_f$ (kW)	$\dot{E}x_p$ (kW)	$\dot{C}_p$ (USD/h)	$\dot{C}_f$ (USD/h)	$\dot{Z}_k$ (USD/h)	$\dot{C}_{D,k}$ (USD/h)	f (%)	r_k (%)
Gas Comp. 1	1374	1228	22.56	22.52	0.0387	2.386	1.59	12.1
Intercooler	240.1	127.1	4.431	4.41	0.0212	2.076	1.01	89.9
Gas Comp. 2	1464	1305	24.03	24.00	0.0387	2.601	1.46	12.3
Comb. chamber	7688	4066	53.68	53.67	0.0109	25.29	0.04	89.1
Gas Turbine	5012	4617	75.68	75.55	0.1236	5.954	2.03	8.7
HRS1	961.8	287.6	14.51	14.50	0.0083	10.16	0.08	234.6
Separator	32,596	32,595	-	-	-	-	-	-
Kalina Turbine	177.9	153	10.01	9.798	0.2165	1.372	13.63	18.9
LTR	13.03	7.848	0.7256	0.718	0.0078	0.2854	2.67	67.8
HTR	20.57	12.62	1.142	1.133	0.0088	0.4382	1.97	64.3
TEG	93.67	67.34	5.225	5.160	0.0643	2.826	2.22	40.8

Table 6. *Cont.*

Component	$\dot{E}x_f$ (kW)	$\dot{E}x_p$ (kW)	$\dot{C}_p$ (USD/h)	$\dot{C}_f$ (USD/h)	$\dot{Z}_k$ (USD/h)	$\dot{C}_{D,k}$ (USD/h)	f (%)	r_k (%)
Kalina Pump	6.508	5.25	0.4339	0.426	0.0079	0.0823	8.75	26.3
Valve	11420	11419	-	-	-	-	-	-
HRS2	339.1	173.3	5.132	5.112	0.0203	0.5846	3.36	96.5
ORC Turbine	260.8	225.3	8.695	8.488	0.2069	1.154	15.02	18.6
ORC Pump	15.83	12.59	0.6214	0.611	0.0106	0.125	1.72	27.9
Condenser	52.12	38.13	0.0470	0.033	0.0991	0.4555	17.87	97.67
PEM	432.3	217.4	7.538	7.085	0.4530	3.522	11.40	111.5

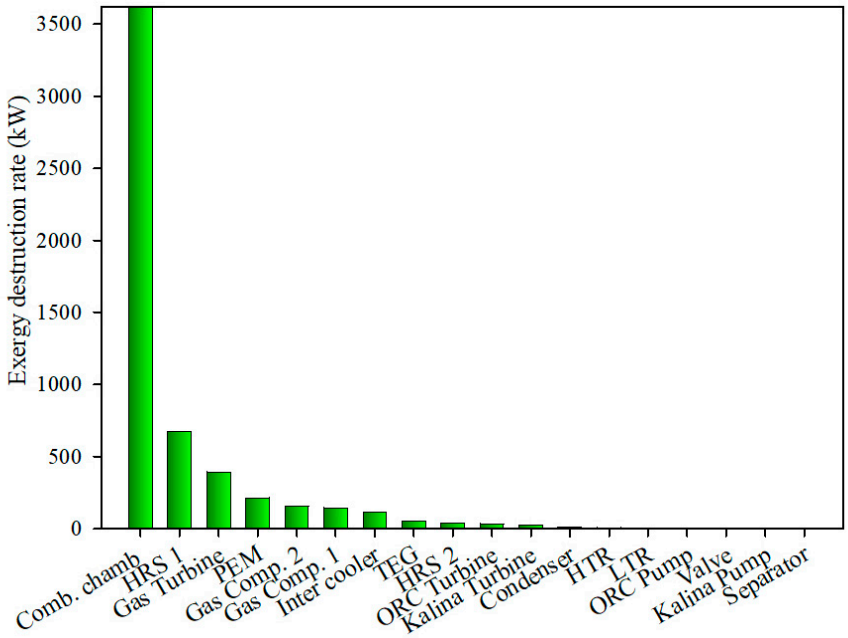

(**a**)

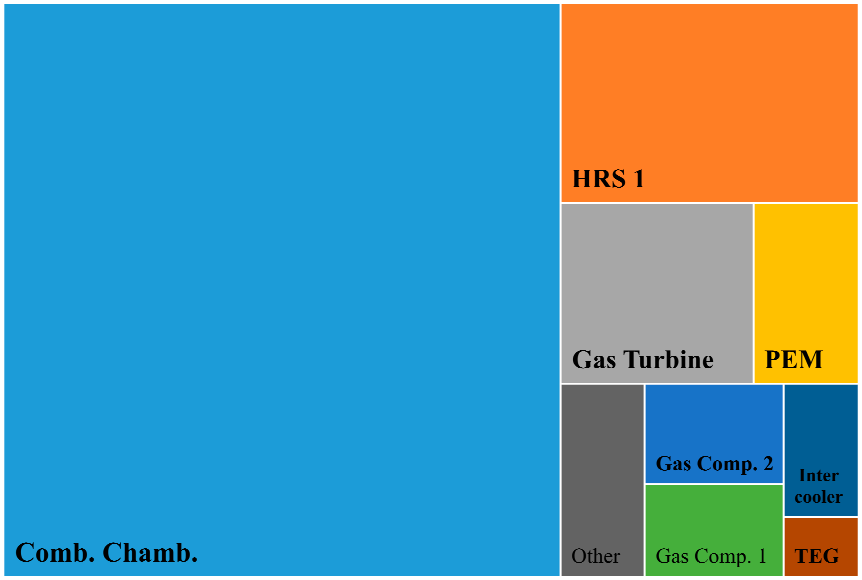

(**b**)

Figure 2. The exergy destruction rate of the IGT/ORC-KC system: (**a**) real values, (**b**) percent of exergy destruction.

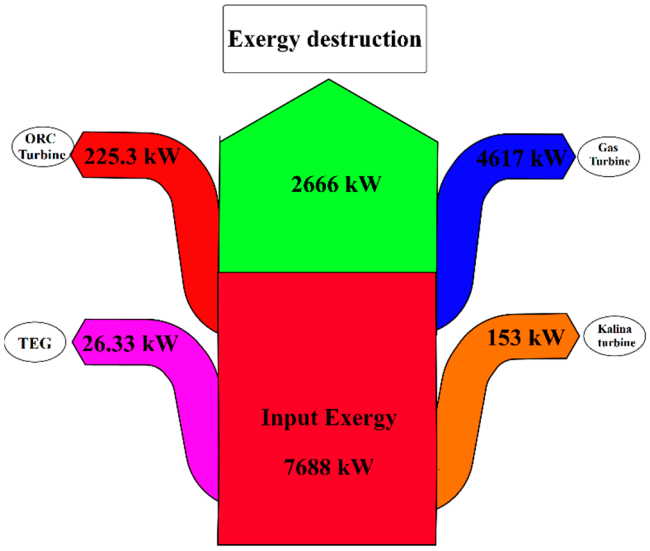

Figure 3. The exergy flow for the proposed system (IGT/ORC-KC).

The exergo-economic factor is also listed in the penultimate column. A high value of each component reflects the high investment cost compared to other costs. Therefore, to enhance the efficiency, the investment cost of the elements must be increased such as the combustion chamber and HRS1, which have lower values. According to the data presented in Table 6, the electrolyzer also has a higher purchase cost rate among all cycle equipment.

4.2.2. Exergo-Environment

This section describes the results of the exergo-environmental analysis for the IGT/ORC-KC plant. To accurately analyze the environmental influences of a system, which includes analyzing the cost and effects of equipment construction, maintenance, and restoration, the exergo-environmental balance is performed. Table 7 shows the results of solving the exergo-environmental equations, which will be used in future analyses and in calculating the environmental indicators.

Table 7. Exergo-economic and exergo-environmental properties of IGT/ORC-KC at different points.

Stream	Fluid	C USD/kWh	$\dot{C}$ (USD/h)	b mPts/kJ	$\dot{B}$ mPts/s
1	Air	0	0	0	0
2	Air	0.04709	1.796	0.01722	0.6566
3	Air	0.01837	18.15	0.007141	7.056
4	Air	0.01839	42.18	0.007152	16.4
5	Air	0.01597	95.87	0.005879	37.39
6	Air	0.01597	20.31	0.005879	7.922
7	Air	0.01597	5.814	0.005879	2.268
8	Air	0.01507	0.7022	0.005879	0.2738
9	NH_3H_2O	0.05508	2425	0.02143	943.7
10	NH_3H_2O	0.05508	1795	0.02143	698.6
11	NH_3H_2O	0.05508	1786	0.02143	694.7
12	NH_3H_2O	0.05509	2415	0.02144	939.5
13	NH_3H_2O	0.05509	2414	0.02144	939.2
14	NH_3H_2O	0.05509	2409	0.02144	937.2
15	NH_3H_2O	0.05509	2409	0.02144	937.4
16	NH_3H_2O	0.0551	2410	0.02144	937.6
17	NH_3H_2O	0.05511	2411	0.02144	938.1
18	NH_3H_2O	0.05508	630.1	0.02143	245.2

Table 7. *Cont.*

Stream	Fluid	C USD/kWh	$\dot{C}$ (USD/h)	b mPts/kJ	$\dot{B}$ mPts/s
19	NH_3H_2O	0.05508	629	0.02143	244.7
20	NH_3H_2O	0.05509	629	0.02143	244.7
21	Water	0	0	0	0
22	Water	0.05509	0.8838	0.02144	0.3439
23	Isobutene	0.03255	18.37	0.0126	7.109
24	Isobutene	0.03255	9.88	0.0126	3.824
25	Isobutene	0.03255	8.184	0.0126	3.167
26	Isobutene	0.03335	8.805	0.01287	3.398
27	Isobutene	0.03384	13.24	0.01307	5.113
28	Water	0	0	0	0
29	Water	0.04709	1.796	0.01722	0.6566

Table 8 lists the results of the exergo-environmental indicators. As can be seen, for the studied equipment, the ECO99 index (a damage-oriented method for life cycle impact assessment) associated with the combustion chamber and HRS1 is much higher than the rest of the equipment. Table 8 also shows the environmental cost rate of exergy destruction ($B_{D,k}$). In the previous cases, the combustion chamber had the most exergy destruction and cost. Yet in this case, the cost of the environmental influence rate of HRS1 and the combustion chamber is higher than that of all the equipment. However, the highest environmental cost is imposed on the studied system by HRS1. Corresponding to the exergo-economic examination, the amounts of the parameters of r_b (relative environmental influence difference) and f_b (exergo-environmental impact factor) have also been calculated.

Table 8. The exergo-environmental indicators for the suggested system.

Element	b_p (mpts/kJ)	b_f (mpts/kJ)	ECO 99 Indicator (pts)	$\dot{B}_{D,k}$ (mpts/s)	$\dot{Y}_k$ (mpts/s)	f_b (%)	r_b (%)
Gas Comp. 1	0.007141	0.006383	955.72	0.929	0.001746	0.1875	11.88
Intercooler	0.01349	0.007141	192.70	0.807	0.000352	0.043	88.99
Gas Comp. 2	0.00716	0.006383	955.72	1.013	0.001746	0.1721	12.18
Comb. chamber	0.005162	0.002893	1782	0.459	0.003255	0.7042	78.41
Gas Turbine	0.006383	0.005879	1168	2.322	0.002133	0.091	8.56
HRS1	0.01967	0.005879	1761	3.964	0.003216	0.081	234.6
Separator	0.04286	0.02143	-	-	-	-	-
Kalina Turbine	0.02492	0.02143	97.09	0.534	0.000177	0.033	16.29
LTR	0.03559	0.02144	22.80	0.111	0.000041	0.0374	66.05
HTR	0.03495	0.02143	43.37	0.111	0.000079	0.071	63.09
TEG	0.02981	0.02144	10.33	1.100	0.000018	0.001	28.11
Kalina Pump	0.03089	0.02492	0.0039	0.031	7.27×10^{-9}	2.32×10^{-5}	23.96
Valve	-	-	-	-	-	-	-
HRS2	0.01152	0.005879	1255	0.228	0.002292	0.995	95.95
ORC Turbine	0.01458	0.0126	128.81	0.447	0.000235	0.052	15.75
ORC Pump	0.01833	0.01458	0.0093	0.047	1.693×10^{-8}	3.585×10^{-5}	25.72
Condenser	0.01722	0.0126	12.75	0.176	0.000023	0.013	36.71
PEM	0.01269	0.006383	2.09	1.371	0.000003	0.00027	98.82

4.3. Comparison Results

In this research, three different systems have been compared. In the past sections, the suggested system was fully examined. In this section, a comparison is presented between the basic system (cycle 1); and cycle 2, in which a Kalina cycle is added to the downstream of the basic cycle; and the proposed cycle. Figure 4 compares the amount of net output work from the systems in the exergy destruction of the three studied systems. It is observed that system 3 has the highest exergy destruction rate due to the fact that it has more subsystems

while each has its exergy destruction rate. The results show that cycle 3 has 24.6% higher exergy destruction than cycle 1.

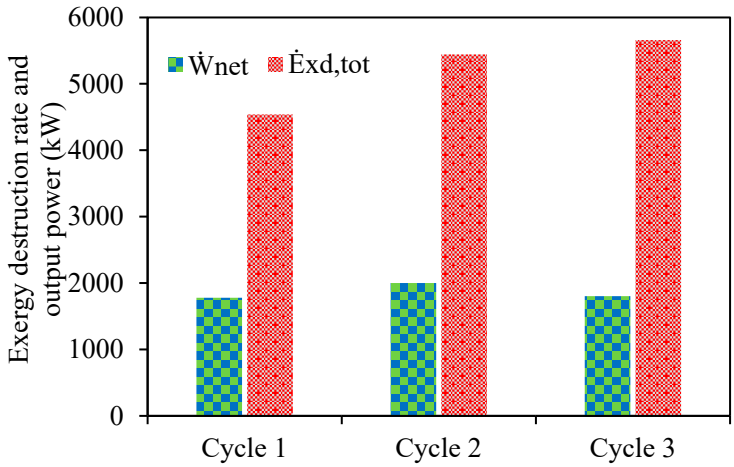

Figure 4. The net output power and exergy destruction rates of the three cycles.

Compared to the other systems, cycle 2 has the highest net output power. The output power of cycle 2 is 11% higher than that of cycle 3. Comparing the energy efficiencies in the three systems, it is evident that system 3 has the highest energy efficiency (Figure 5). The different systems show different results in terms of exergy efficiency. Regarding the exergy efficiency of system 3, it can be argued that because a part of high-quality energy enters the RO system in the form of electrical power, which is removed from the numerator in the efficiency calculation, the exergy efficiency of system 3 is lower than that of system 2. However, regarding the energy efficiency based on the definitions, this reduction is not observed.

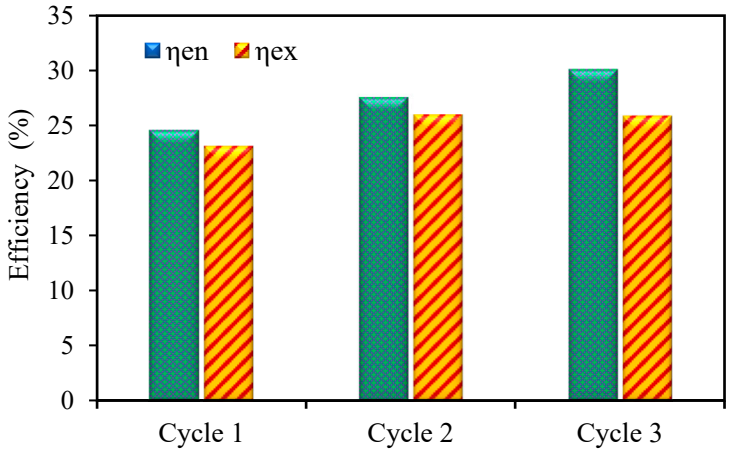

Figure 5. Energy and exergy efficiency of the designed cycles.

4.4. ANN Optimization

Here, the main goal is to find the objective function, namely, exergy efficiency, cost of product, and total environmental impact as functions of the decision variables, namely, compressor pressure ratio (r_p), inlet temperature to gas turbine (T_5), inlet pressure to the ORC turbine (P_{23}), and inlet pressure to the separator (P_9).

4.4.1. Neural Network

By using the technique of neural networks, objective functions can be obtained based on decision variables and can help in multi-objective optimization [32,33]. In this research,

three goals have been assumed, which can be achieved by using the artificial neural network technique. The decision variables, according to which the objective functions are changed, are the compressor pressure ratio, gas turbine inlet temperature, ORC turbine inlet pressure, and Kalina cycle separator inlet pressure. The goal is to find each of the objective functions as a function of four input parameters. Here, the steps to find the energy efficiency function are described, but the same procedure must be followed for the other functions. Figure 6 shows a network with two layers including a hidden layer and a feed-forward neural network for the efficiency function. There are 10 neurons in the hidden layer.

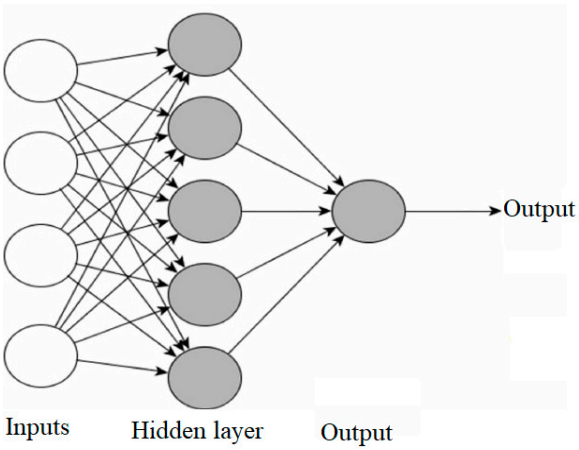

Figure 6. Network structure with a hidden layer.

About 70% of the data are used for training and 30% are used for testing the network. In order to see how the performance of the network improves during training, a logarithmic scale graph is prepared in Figure 7. As can be seen, the value of mean square error has decreased rapidly with network training.

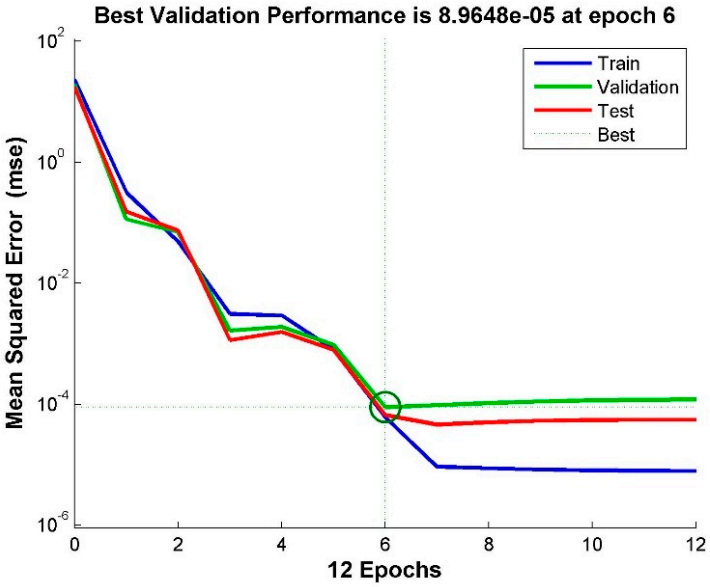

Figure 7. Mean squared error for training and testing data.

It also shows the regression diagram of the network outputs according to the actual values that are the target. The linear form of this graph with a slope of 1 indicates that the network is well fitted to the existing data (Figure 8).

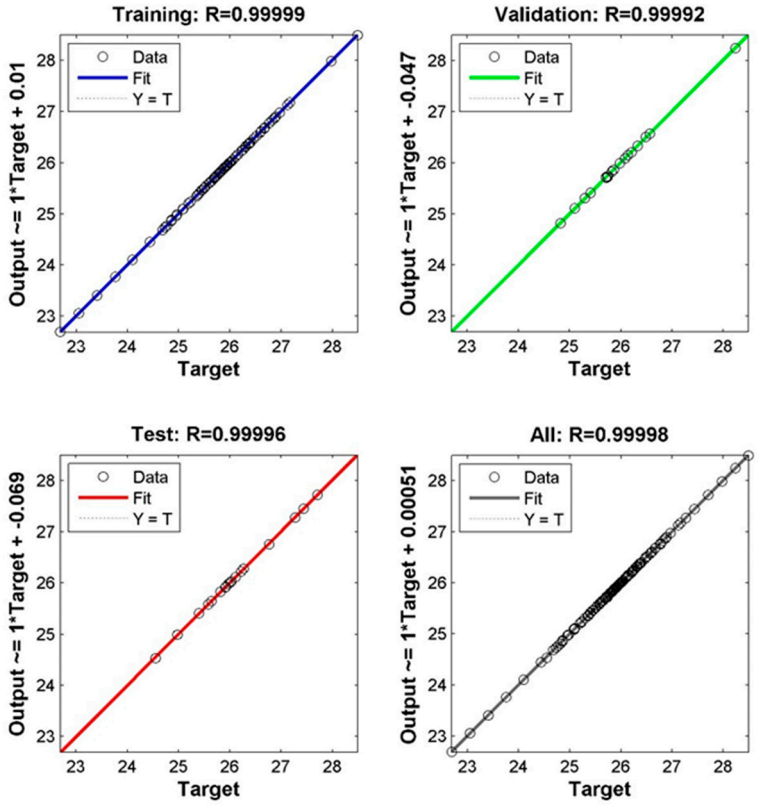

Figure 8. Regression diagram for real data and neural network data.

Another criterion that can be considered to verify the network is the histogram error diagram. Figure 9 shows the error size and the error distribution in such a way that the created network is well fitted to the data.

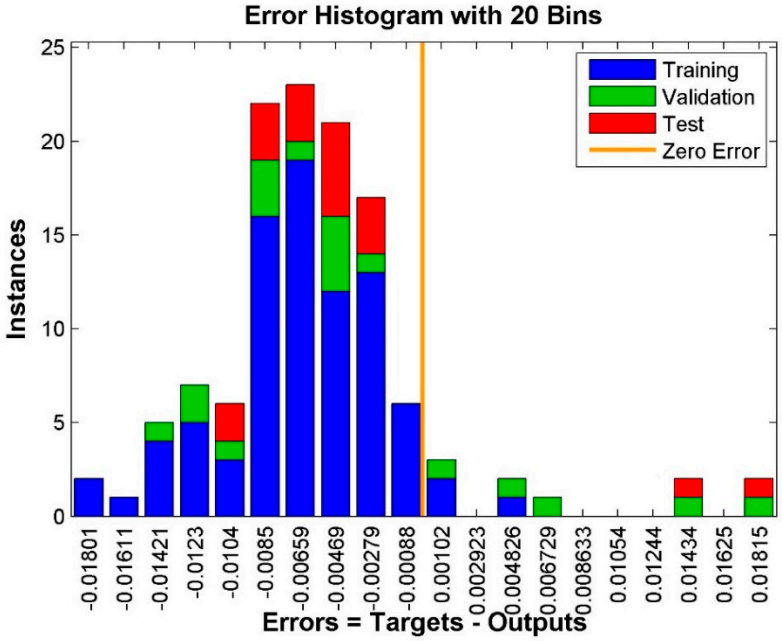

Figure 9. Error histogram for validation, test, and training data.

The above approach can also be applied for the cost of product and environmental impact of exergy destruction to obtain the objective functions.

4.4.2. Multi-Objective Optimization

In this section, the optimization outcomes of the studied system are given. Optimization has been performed for three objective functions, i.e., energy efficiency, cost of products, and environmental influences of exergy destruction. In this optimization approach, energy efficiency should be maximized, the cost of products should be minimized, and the environmental influences of exergy destruction should be minimized. Also, four parameters affecting the performance of the system, i.e., compressor pressure ratio (r_p), inlet temperature to the gas turbine (T_5), inlet pressure to the ORC turbine (P_{23}), and inlet pressure to the separator (P_9), have been chosen as decision parameters. The range of decision variables is given in Table 9. After implementing the multi-objective optimization according to the genetic algorithm, the optimal points of the plant are given in the Pareto diagram, which is a three-dimensional diagram as presented in Figure 10. Based on the definition of the Pareto diagram, all points in the given space can be selected as optimal points. However, different methods can be used to find a point among the optimal points.

Table 9. Specifications of various points on the Pareto diagram.

		Point A	Point B	Point C	Point T
Decision variables	r_p	9.00	10.43	9.03	9.02
	T_5	844.63	844.32	757.73	840.78
	P_{23}	11.61	12.00	12.00	11.75
	P_9	22.04	22.33	26.56	22.62
Objective functions	Exergy efficiency	29.61	27.89	26.27	29.50
	Cost of product	0.309	0.30	0.3472	0.31
	Environmental effects of exergy destruction	13.30	13.46	12.80	13.22

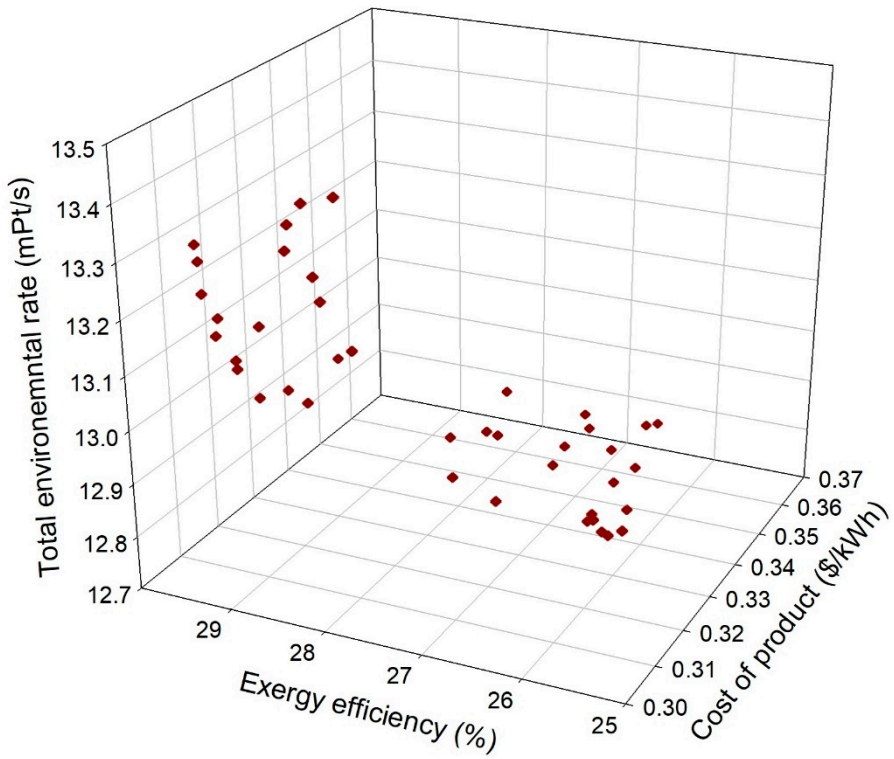

Figure 10. Pareto diagram for multi-objective optimization based on the three defined targets.

The TOPSIS method is a multi-criteria decision-making method that deals with the ranking of options. In this method, two concepts of "ideal solution" and "similarity to

ideal solution" are used. An ideal solution is a solution that is the best in every way, which generally does not exist in practice, and we try to obtain a solution that is close to the ideal solution. In order to measure the similarity of a plan to the ideal and anti-ideal solutions, the distance of that plan from the ideal and anti-ideal solutions is measured. Then the options are evaluated and ranked based on the ratio of the distance from the anti-ideal solution to the total distance from the ideal and anti-ideal solutions.

Using the TOPSIS technique, an optimal state can be obtained among the points suggested in the Pareto diagram with the same characteristics as those given in Table 9 for the T point. Points A, B, and C, are associated with single-objective optimization based on the exergy efficiency, cost of products, and environmental influences of exergy destruction.

5. Conclusions

In this study, three configurations based on gas turbines were investigated to present a system with the best performance and lowest waste. In this study, 4E investigation for all three systems has been implemented for a detailed review of the studied systems and a comprehensive evaluation. In addition, a comparison between the designed systems has been applied based on energy, exergy, and exergo-environmental criteria. To sum, the most important results of this research are reported as follows:

- The results of the energy and exergy examinations present that the suggested system with the Kalina cycle and thermoelectric together with the electrolyzer produces 1800 kW power and has energy and exergy efficiencies of 30% and 25.8% with 0.22 kg/day of hydrogen production.
- In the suggested system (cycle 3), the combustion chamber and HRS1 with 3622 kW and 674.2 kW have the highest destruction values.
- The results of the exergo-economic examination state that the parameter of r_k has a high value for HRS1.
- The results related to the calculation of the exergo-economic factor represent that in order to increase the performance of the suggested system, the investment cost of equipment such as the combustion chamber and HRS1 should be increased.
- The results of the exergo-environmental examination also indicate that the highest environmental cost is brought to the suggested equipment system by HRS1.
- The results of the comparative investigation show that the suggested system has the highest energy efficiency compared to the other systems, while its exergy destruction is the highest.
- The results of this research can be applied in designing the gas turbine system with minimum waste and maximum efficiency from primary energy sources.

Funding: This study is supported via funding from Prince Sattam bin Abdulaziz University project number (PSAU/2023/R/1444).

Data Availability Statement: Data are contained within the article.

Acknowledgments: The author acknowledged the financial support from Prince Sattam bin Abdulaziz University project number (PSAU/2023/R/1444).

Conflicts of Interest: The author declares no conflict of interest.

References

1. Loni, R.; Najafi, G.; Bellos, E.; Rajaee, F.; Said, Z.; Mazlan, M. A review of industrial waste heat recovery system for power generation with Organic Rankine Cycle: Recent challenges and future outlook. *J. Clean. Prod.* **2020**, *287*, 125070. [CrossRef]
2. Bozgeyik, A.; Altay, L.; Hepbasli, A. Energetic, exergetic, exergoeconomic, environmental and sustainability analyses of a solar, geothermal and biomass based novel multi-generation system for production of power, hydrogen, heating, cooling and fresh water. *Process. Saf. Environ. Prot.* **2023**, *177*, 400–415. [CrossRef]
3. Al-Ali, M.; Dincer, I. Energetic and exergetic studies of a multigenerational solar–geothermal system. *Appl. Therm. Eng.* **2014**, *71*, 16–23. [CrossRef]

4. Musharavati, F.; Khanmohammadi, S.; Pakseresht, A.; Khanmohammadi, S. Waste heat recovery in an intercooled gas turbine system: Exergo-economic analysis, triple objective optimization, and optimum state selection. *J. Clean. Prod.* **2020**, *279*, 123428. [CrossRef]
5. Nguyen, H.T.; Battula, S.; Takkala, R.R.; Wang, Z.; Tesfatsion, L. An integrated transmission and distribution test system for evalu-ation of transactive energy designs. *Appl. Energy* **2019**, *240*, 666–679.
6. Yi, S.; Lin, H.; Abed, A.M.; Shawabkeh, A.; Marefati, M.; Deifalla, A. Sustainability and exergoeconomic assessments of a new MSW-to-energy incineration multi-generation process integrated with the concentrating solar collector, alkaline electrolyzer, and a reverse osmosis unit. *Sustain. Cities Soc.* **2023**, *91*, 104412. [CrossRef]
7. Mahdavi, N.; Mojaver, P.; Khalilarya, S. Multi-objective optimization of power, CO_2 emission and exergy efficiency of a novel solar-assisted CCHP system using RSM and TOPSIS coupled method. *Renew. Energy* **2021**, *185*, 506–524. [CrossRef]
8. Leveni, M.; Manfrida, G.; Cozzolino, R.; Mendecka, B. Energy and exergy analysis of cold and power production from the geothermal reservoir of Torre Alfina. *Energy* **2019**, *180*, 807–818. [CrossRef]
9. Hosseini, S.E. Design and analysis of renewable hydrogen production from biogas by integrating a gas turbine system and a solid oxide steam electrolyzer. *Energy Convers. Manag.* **2020**, *211*, 112760. [CrossRef]
10. Nami, H.; Mohammadkhani, F.; Ranjbar, F. Utilization of waste heat from GTMHR for hydrogen generation via combination of organic Rankine cycles and PEM electrolysis. *Energy Convers. Manag.* **2016**, *127*, 589–598. [CrossRef]
11. Nami, H.; Akrami, E. Analysis of a gas turbine based hybrid system by utilizing energy, exergy and exergoeconomic methodologies for steam, power and hydrogen production. *Energy Convers. Manag.* **2017**, *143*, 326–337. [CrossRef]
12. Singh, R.; Singh, O. Comparative study of combined solid oxide fuel cell-gas turbine-Organic Rankine cycle for different working fluid in bottoming cycle. *Energy Convers. Manag.* **2018**, *171*, 659–670. [CrossRef]
13. Manesh, M.H.K.; Ghorbani, S.; Blanco-Marigorta, A.M. Optimal design and analysis of a combined freshwater-power generation system based on integrated solid oxide fuel cell-gas turbine-organic Rankine cycle-multi effect distillation system. *Appl. Therm. Eng.* **2022**, *211*, 118438. [CrossRef]
14. Gholamian, E.; Hanafizadeh, P.; Habibollahzade, A.; Ahmadi, P. Evolutionary based multi-criteria optimization of an integrated energy system with SOFC, gas turbine, and hydrogen production via electrolysis. *Int. J. Hydrog. Energy* **2018**, *43*, 16201–16214. [CrossRef]
15. Shamoushaki, M.; Ehyaei, M.; Ghanatir, F. Exergy, economic and environmental analysis and multi-objective optimization of a SOFC-GT power plant. *Energy* **2017**, *134*, 515–531. [CrossRef]
16. Hemadri, V.B.; Subbarao, P. Thermal integration of reheated organic Rankine cycle (RH-ORC) with gas turbine exhaust for maximum power recovery. *Therm. Sci. Eng. Prog.* **2021**, *23*, 100876. [CrossRef]
17. El-Sattar, H.A.; Kamel, S.; Vera, D.; Jurado, F. Tri-generation biomass system based on externally fired gas turbine, organic rankine cycle and absorption chiller. *J. Clean. Prod.* **2020**, *260*, 121068. [CrossRef]
18. Roy, D.; Samanta, S.; Ghosh, S. Techno-economic and environmental analyses of a biomass based system employing solid oxide fuel cell, externally fired gas turbine and organic Rankine cycle. *J. Clean. Prod.* **2019**, *225*, 36–57. [CrossRef]
19. Cao, Y.; Mihardjo, L.W.; Dahari, M.; Tlili, I. Waste heat from a biomass fueled gas turbine for power generation via an ORC or compressor inlet cooling via an absorption refrigeration cycle: A thermoeconomic comparison. *Appl. Therm. Eng.* **2020**, *182*, 116117. [CrossRef]
20. Liu, Z.; Ehyaei, M.A. Thermoeconomic and exergoenvironmental assessments of a combined micro-gas turbine and superheated Kalina cycles for cogeneration of heat and electrical power using biomass. *Int. J. Environ. Sci. Technol.* **2022**, *19*, 11233–11248. [CrossRef]
21. Ebrahimi-Moghadam, A.; Farzaneh-Gord, M.; Moghadam, A.J.; Abu-Hamdeh, N.H.; Lasemi, M.A.; Arabkoohsar, A.; Alimoradi, A. Design and multi-criteria optimisation of a trigeneration district energy system based on gas turbine, Kalina, and ejector cycles: Exergoeconomic and exergoenvironmental evaluation. *Energy Convers. Manag.* **2020**, *227*, 113581. [CrossRef]
22. Du, Y.; Jiang, N.; Zhang, Y.; Wang, X.; Zhao, P.; Wang, J.; Dai, Y. Multi-objective optimization of an innovative power-cooling integrated system based on gas turbine cycle with compressor inlet air precooling, Kalina cycle and ejector refrigeration cycle. *Energy Convers. Manag.* **2021**, *244*, 114473. [CrossRef]
23. Mohammadkhani, F.; Yari, M.; Ranjbar, F. A zero-dimensional model for simulation of a Diesel engine and exergoeconomic analysis of waste heat recovery from its exhaust and coolant employing a high-temperature Kalina cycle. *Energy Convers. Manag.* **2019**, *198*, 111782. [CrossRef]
24. Çengel, Y.A.; Boles, M.A. *Thermodynamics: An Engineering Approach*, 8th ed.; McGraw-Hill Education: New York, NY, USA, 2004.
25. Bejan, A.; Tsatsaronis, G.; Moran, M.J. *Thermal Design &Optimization*; John Wiley & Sons: Hoboken, NJ, USA, 1996; p. 542.
26. Meyer, L.; Tsatsaronis, G.; Buchgeister, J.; Schebek, L. Exergoenvironmental analysis for evaluation of the environmental impact of energy conversion systems. *Energy* **2009**, *34*, 75–89. [CrossRef]
27. SimaPro | LCA Software for Informed-Change Makers. Available online: https://network.simapro.com/ (accessed on 20 September 2023).
28. Gill, E.Z.; Ratlamwala, T.A.H.; Hussain, G.; Alkahtani, M. Energy, exergy, exergo-economic and exergo-environmental analyses of solar based hydrogen generation system. *Int. J. Hydrogen Energy* **2021**, *46*, 29049–29064. [CrossRef]
29. Boyano, A.; Blanco-Marigorta, A.; Morosuk, T.; Tsatsaronis, G. Exergoenvironmental analysis of a steam methane reforming process for hydrogen production. *Energy* **2011**, *36*, 2202–2214. [CrossRef]

30. Mohammadi, A.; Kasaeian, A.; Pourfayaz, F.; Ahmadi, M.H. Thermodynamic analysis of a combined gas turbine, ORC cycle and absorption refrigeration for a CCHP system. *Appl. Therm. Eng.* **2017**, *111*, 397–406. [CrossRef]
31. Fallah, M.; Mahmoudi, S.M.S.; Yari, M.; Ghiasi, R.A. Advanced exergy analysis of the Kalina cycle applied for low temperature enhanced geothermal system. *Energy Convers. Manag.* **2016**, *108*, 190–201. [CrossRef]
32. Kong, C.K.; Low, L.E.; Siew, W.S.; Yap, W.H.; Khaw, K.Y.; Ming, L.C.; Mocan, A.; Goh, B.H.; Goh, P.H. Biological activities of snowdrop (*Galanthus* spp., Family Amaryllidaceae). *Front. Pharmacol.* **2021**, *11*, 552453. [CrossRef]
33. Ahmed, H.A.; Ali, P.J.M.; Faeq, A.K.; Abdullah, S.M. An Investigation on Disparity Responds of Machine Learning Algorithms to Data Normalization Method. *ARO Sci. J. Koya Univ.* **2022**, *10*, 29–37. [CrossRef]